Table S1: Characteristics of patients in the discovery cohort

Patient ID	Response	Sex	Age (yrs)	WHO class.	Mutations (VAF %)	Karyotype	BM blasts (%)	Hb (g/L)	ANC (×10⁹/L)	Platelet count (×10⁹/L)	IPSS-R score in MDS	IPSS-R in MDS
V1788	RD	M	81	MDS-EB-2	*TP53* (59) *SF3B1* (40)	Complex	13.6	66	0.22	78	9.5	very high
V1456	RD	F	75	MDS-MLD	*SF3B1* (39) *TET2* (46) *CUX1*(49)	46,XX[1], 46,XX,idic(X)(q13)[8], 46,XX,idic(X)(q13), +idic(X)(q13) [20], 46,XX,idic(X)(q13), +idic(X)(q13), +idic(X)(q13)[1]	7	88	0.31	27	6.5	very high
V839	RD	F	78	MDS-EB-2	*DNMT3A* (44) *RUNX1* (26)	46,XX[3]; 47,XX,del(5)(q31),+8[19]	7.7	88	1.97	90	4.5	intermediate
V406	RD	M	67	MDS-EB-2	*SF3B1* (27)	46,XY[8]; 47,XY,del(5)(q31),+8[14]	18	89	0.61	74	6	high
V574	RD	F	77	AML-MRC	*JAK2* (41)	46,XX[5]; 46,XX,del(5)(q31.2q33.1)[18]	24	109	11.80	578	NA	NA
V538	RD	F	82	MDS-EB-1	*DNMT3A*(46) *BCOR* (40)	46,XX[5]; 46,XX,del(5)(q22q32.2)[17]	4.6	107	3.27	124	2	low
V624	RD	F	74	MDS-EB-2	*SF3B1*(42) *TP53*(47) *RUNX1* (42)	46,XX,del(5)(q13.2q34)[6]	18	82	0.40	80	6	high
V1884	RD	F	73	MDS-EB-2	*TP53* (36) *TP53*(40)	Complex	18.2	91	0.34	NA	9.5	very high
V655	RD	F	63	MDS-EB-2	*TP53* (69)	Complex	15.6	95	0.44	65	9	very high
V1279	RD	M	65	MDS-EB-2	*TET2* (19) *TET2* (22) *EZH2* (6) *ZRSR2* (68)	46,XY[22]	11	117	0.24	172	4.5	intermediate
V716	SD	M	63	MDS-EB-2	*SF3B1*(18)	46,XY[1]; 45,XY,del(5)(q12q33.3), dic(7;11)(p12;q13)[23]	14.2	117	2.68	51	4.5	intermediate
V1874	SD	M	74	AML-MRC	*0*	46,XY[22]	27.4	127	1.32	81	NA	NA
V1441	SD	F	70	MDS-EB-2	*RUNX1* (30) *TET2* (6) *BCOR* (28)	46,XX, t(9;21) [14]	10.2	86	0.54	53	5	high

V1337	SD	M	44	MDS-EB-2	*WT1* (7) *TP53* (3)	46,XY[16], 46,XY,t(3;21)(q11.2;q22), del(7)(q22)[5]	6.6	127	1.82	70	3.5	intermediate
V1394	SD	M	69	MDS-EB-2	*NRAS* (46) *ETV6* (49) *ASXL1* (38) *STAG2* (90) *PHF6* (96) *GATA2* (43)	46,XY[20]	12.2	101	3.71	37	5	high
V1592	SD	F	64	MDS-EB-2	*TET2* (45) *RUNX1* (45) *ASXL1* (50) *EZH2* (49) *PHF6* (45)	46,XX[5]; 47,XX,+8[20]	13	100	4.97	26	6	high
V456	PD	F	68	MDS-EB-2	*0*	46,XX[15]	18.4	90	1.15	141	5	high
V1857	PD	F	73	MDS-EB-2	*DNMT3A* (41)	46,XX[22]	17	111	0.93	20	5.5	high
V714	PD	M	70	AML-MRC	*CBL* (8) *NRAS*(8)	46,XY[13]	27	91	0.06	34	NA	NA
V777	PD	M	68	AML-MRC	*0*	46,XY[14]	27	106	1.73	106	NA	NA
V637	PD	M	65	MDS-EB-2	*0*	47,XY,+11[22]	10	83	0.39	80	6	high
V712	PD	M	67	MDS-EB-2	*SRSF2* (32) *ASXL1* (26) *RUNX1* (30) *BCOR* (6) *STAG2* (6) *STAG2* (5)	46,XY[22]	19.4	97	0.41	45	6.5	very high
V1297	PD	M	68	MDS-EB-2	*TP53* (8)	Complex	10.6	98	0.26	38	8.5	very high
V1554	PD	M	62	AML-MRC	*IDH2* (5) *IKZF1* (22) *STAG2* (6)	46,XY [22], 46,XY,del(5)(q13q33) [2]	26	91	1.02	124	NA	NA
V344	PD	F	64	MDS-EB-2	*TP53* (68) *SF3B1* (40) *DNMT3A* (52)	46,XX[13],del(5)(q15q33.3)[9]	17.2	91	3.56	35	6	high

VAF – variant allele frequency, BM – bone marrow, Hb – hemoglobin, WHO class. – WHO classification, NA – not available

Table S2: Characteristics of patients in the validation cohort

Patient ID	Response	Sex	Age (yrs)	WHO class.	Mutations (VAF %)	Karyotype	BM blasts (%)	Hb (g/L)	ANC (×10⁹/L)	Platelet count (×10⁹/L)	IPSS-R score in MDS	IPSS-R in MDS
P1618	RD	F	65	MDS-MLD	*CSF3R* (22) *DNMT3A* (33) *TP53* (30) *U2AF1* (28)	No metaphases (FISH -7)	2.6	107	0.85	33	5	high
P1648	RD	M	75	MDS-EB-1	*DNMT3A* (9)	NA	9,2	129	2.12	95	NA	NA
P942	RD	F	78	AML-MRC	*DNMT3A* (41)	NA	7.2	77	1,91	120	NA	NA
P1040	RD	M	62	MDS-EB-2	*0*	46,XY[22]	12.8	115	1,53	176	4	intermediate
P2291	RD	F	68	AML-MRC	*TP53* (52) (8) *TET2* (37)	Complex	8.2	91	2.03	72	NA	NA
P1605	SD	F	76	AML-MRC	*IDH2* (26) *DNMT3A* (50)	46,XX[8]	41	86	0.1	76	NA	NA
P1775	SD	M	71	MDS-EB-2	*PTEN* (10)	46,XY[22]	12.6	137	1.68	84	4.5	intermediate
P1824	SD	M	71	MDS-EB-2	*ASXL1 (25)* *RUNX1*(11) *SF3B1 (42)* *ZRSR2 (25)* *STAG2* (35)	46,XY[17]	6.6	88	1.59	216	5	high
P1898	SD	M	80	MDS EB-2	*ASXL1* (6)	46,XY[6]	11	109	0.31	63	5	high
P1836	SD	M	40	MDS-EB-2	*0*	46,XY[6]	19.6	91	0.26	23	6.5	very high
P1357	SD	F	72	MDS-EB-1	*TP53* (18)	Complex	8.6	75	0.53	49	9	very high
P683	SD	M	56	MDS-EB-2	*DNMT3A* (39) *JAK2* (50)	46,XY[22]	10.2	84	4.41	122	5	high
P1371	PD	F	69	AML-MRC	*0*	46, XX [7]	26.6	119	0.77	258	NA	NA
P1564	PD	M	72	AML-MRC	*TP53* (15)	Complex	13.8	77	0.36	29	NA	NA
P1803	PD	M	71	MDS-EB-2	*DNMT3A* (41)	Complex	12.8	79	2.36	34	5.5	high
P689	PD	F	65	AML-MRC	*DNMT3A* (42) *RUNX1* (33) *U2AF1* (38)	No metaphases	15.2	87	0.5	144	NA	NA

P1333	PD	M	66	MDS-EB-1	*SETBP1* (24) *DNMT3A* (26)	No metaphases (FISH-7)	7.4	77	0.39	72	7.5	very high

VAF – variant allele frequency, BM – bone marrow, Hb – hemoglobin, WHO class. – WHO classification, NA – not available

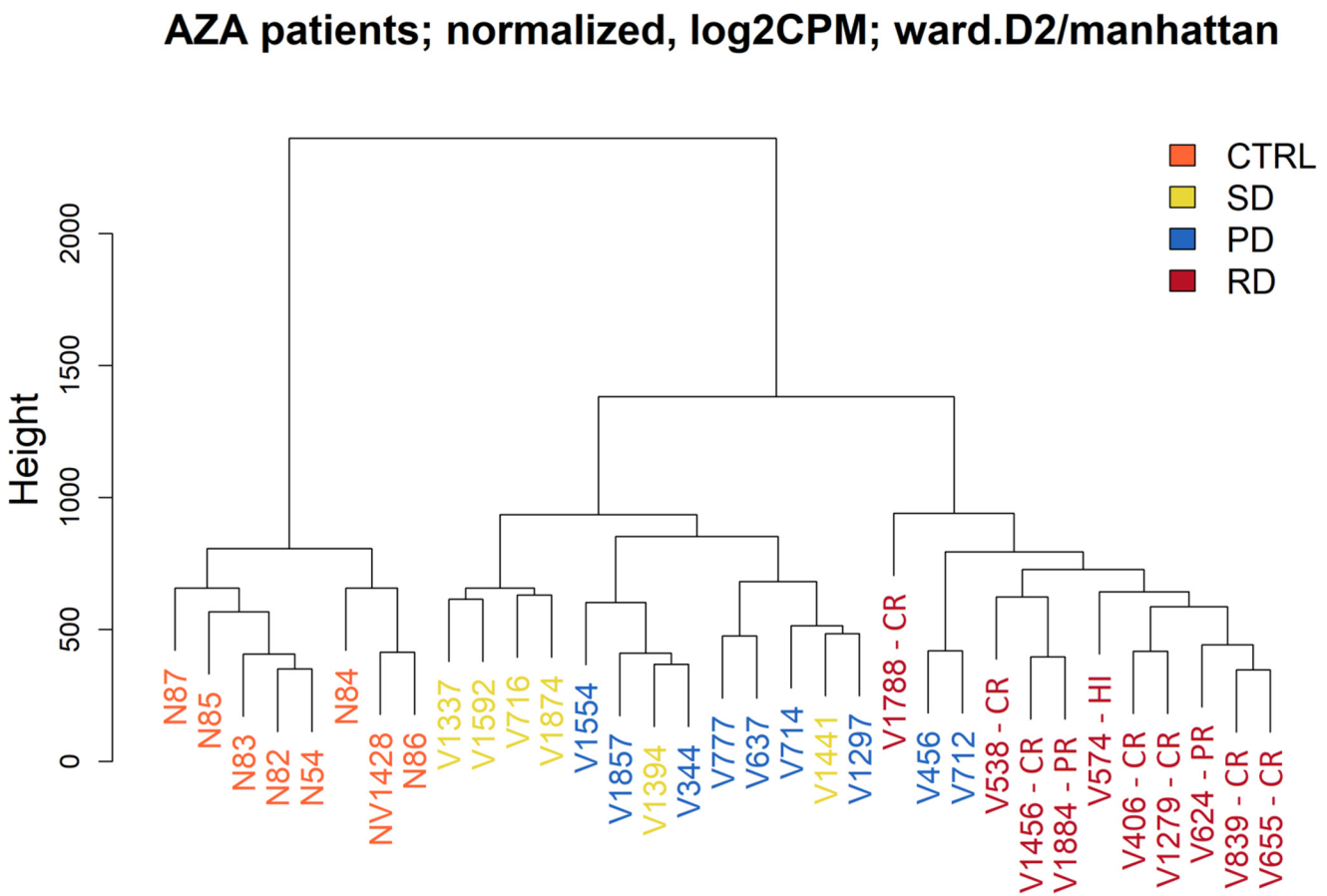

Figure S1: Dendogram obtained from unsupervised hierarchical clustering analysis in patients' discovery cohort (n = 25) and normal controls (n = 8), based on normalized RNA-seq expression data (details are described in the Supplementary Materials and Methods section). Unsupervised hierarchical clustering separated the samples into two main groups, patients and controls. Within the patients' group, the branch of RD patients contains grouped patients with complete remission (CR), partial responses (PR) and hematological improvements (HI).

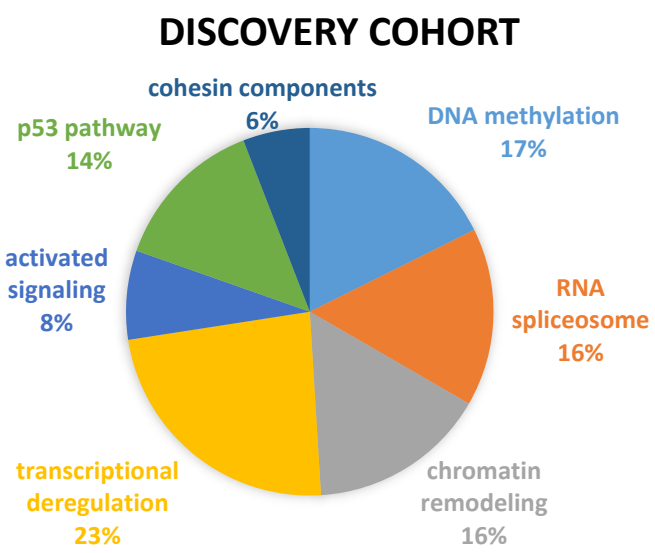

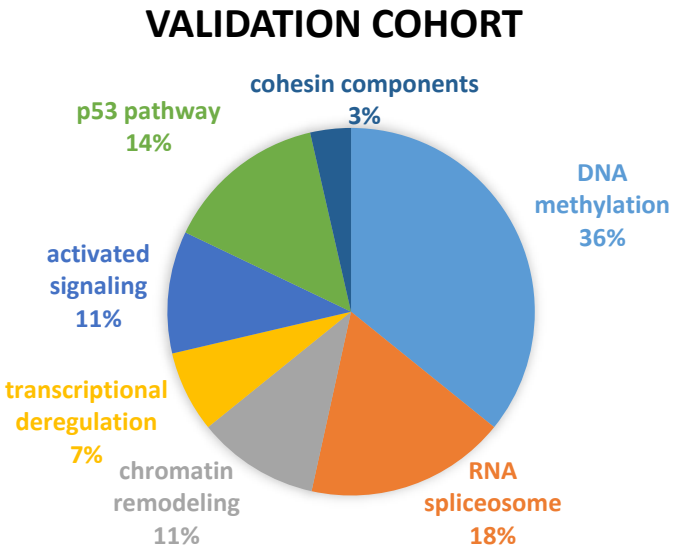

Functional group (frequency, %)	Total (n=42)	Discovery cohort (n=25)	Validation cohort (=17)	*P* value
DNA methylation (*DNMT3A, TET2, IDH1/2*)	19 (45%)	9 (36%)	10 (59%)	0.253
RNA spliceosome (*SF3B1, SRSF2, ZRSR2, U2AF1*)	12 (29%)	8 (32%)	5 (29%)	0.804
Chromatin remodeling (*ASXL1, EZH2, BCOR, SETBP1*)	11 (26%)	8 (32%)	3 (18%)	0.496
Transcriptional deregulation (*RUNX1, WT1, ETV6, CUX1, GATA2, PHF6, IKZF1*)	14 (33%)	12 (48%)	2 (12%)	0.010
Activated signaling (*NRAS, CBL, JAK2, PTEN, CSF3R*)	7 (17%)	4 (16%)	3 (18%)	0.779
p53 pathway (*TP53*)	11 (26%)	7 (28%)	4 (24%)	0.973
Cohesin components (*STAG2*)	4 (10%)	3 (12%)	1 (6%)	0.899

Figure S2: Gene mutational analysis of patients in discovery and validation cohorts. Mutation frequencies are categorized according to functional classification. For mutation analysis methodology see Supplementary Materials and Methods. P of the analysis is the p value of the chi-square test with Yates' correction for small sample sizes.

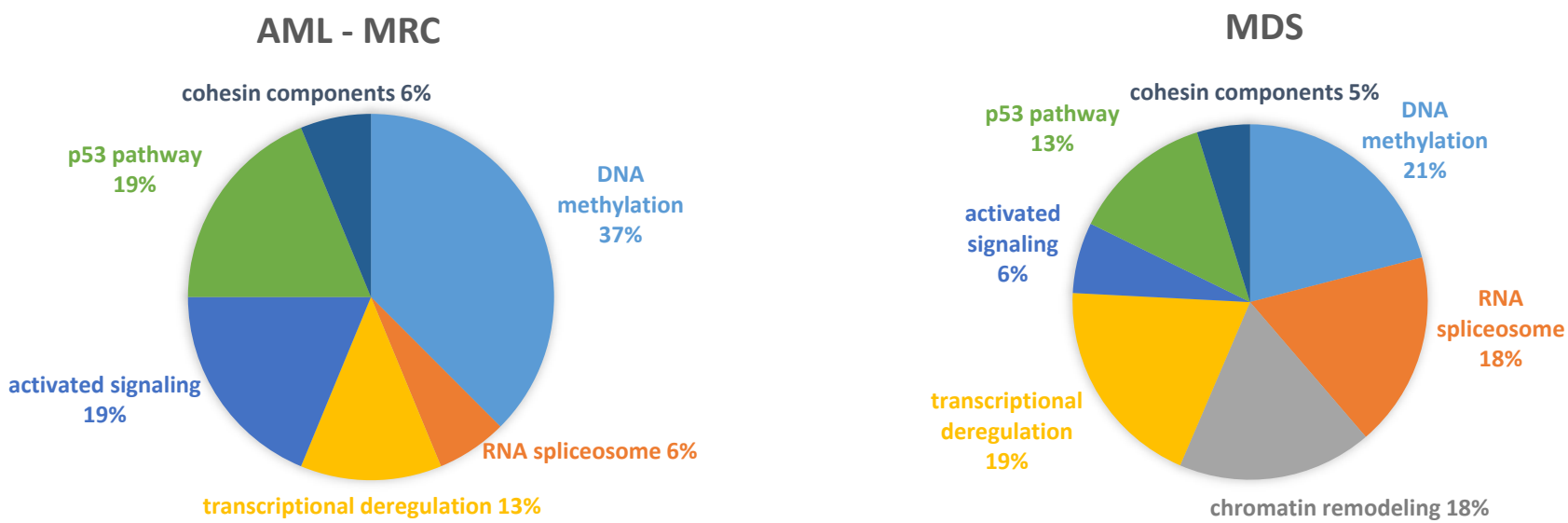

Figure S3: A comparison of mutation frequencies in patients categorized as AML-MRC or MDS within the discovery/validation cohorts. Mutation frequencies are categorized according to the functional classification of respective genes, as described in Figure S2 above.

Table S3: Clinical characteristics of all patients in the study

Parameter	Responders	Stable disease	Progressive disease	p-value[a]
Total, n	15	13	14	
Age (yrs), median (range)	74 (62-82)	70 (40-80)	68 (62-73)	0.14
Patients sex				0.13
Male (%)	5 (33)	9 (69)	9 (64)	
Female (%)	10 (67)	4 (31)	5 (36)	
Bone marrow blasts (%), median (range)	11.0 (2.6-24)	12.2 (6.6-30)	17.1 (7.4-27)	0.08
Hemoglobin (g/dL), median (range)	9.1 (6.6-12.9)	10 (7.5-13.7)	9.1 (7.7-11.9)	0.56
Platelet count ($\times 10^9$/L), median (range)	85 (27-578)	93 (23-216)	59 (20-258)	0.27
ANC ($\times 10^9$/L), median (range)	0.9 (0.2-11.8)	1.6 (0.1-5.0)	0.5 (0.1-3.56)	0.48
Cytogenetic risk[b] (%)				0.51
Very good, Good	6	10	8	
Intermediate	2	1	1	
Poor, Very poor	4	2	3	
Not applicable	3	0	2	
Number of mutations, median (range)	2 (0-6)	2 (0-6)	1 (0-6)	0.47
WHO classification, n				0.31
MDS-MLD	2	0	0	
MDS-EB1	2	1	1	
MDS-EB2	8	10	7	
AML-MRC	3	2	6	
OS since start AZA, median (months)	22.9	47.0	7.6	<0.0001
PFS since start AZA, median (months)	20.8	47.0	3.1	<0.0001

[a] p-values were calculated by Kruskal-Wallis test for continuous variables, Fisher's exact test for categorical variables and Log Rank (Mantel-Cox) test for survival analysis.

[b] The cytogenetic risk was calculated based on the IPSS-R cytogenetic risk groups for MDS and were used also for AML-MRC.

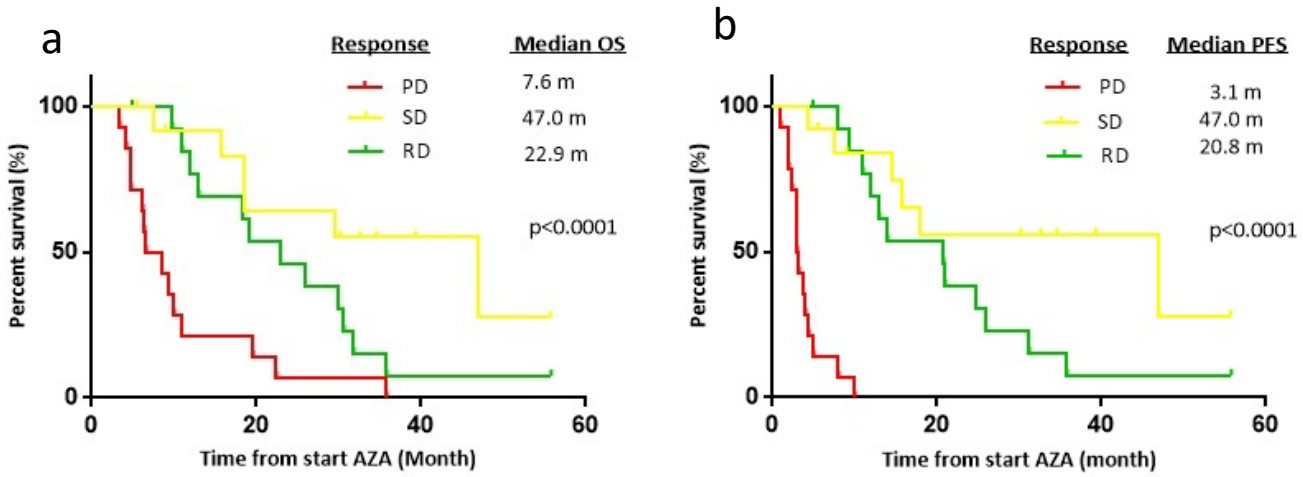

Figure S4: Kaplan–Meier curves of overall survival (OS) and progression-free survival (PFS) in AZA – treated patients divided into three groups according to treatment response status. Patients of discovery and validation cohorts were grouped into progressive disease (PD, n=14), stable disease (SD, n=13) and responders (RD, n=15) by response status. (A) OS in PD, SD and RD patients was 7.6, 47.0 and 22.9 months, respectively (P <0.0001). (B) PFS in PD, SD and RD patients was 3.1, 47.0 and 20.8 months, respectively (P <0.0001).

Table S4: Specification of antibodies used in the study.

ANTIGEN	HOST	CLONALITY	CLONE	DILUTION	PRODUCT N.	COMPANY
IDH1	Rabbit	poly	-	1:1000	ab94571	Abcam
IDH2	Rabbit	mono	EPR7577	1:1000	ab131263	Abcam
pan-acetyl-lysine	Rabbit	poly	-	1:200	ab80178	Abcam
AIF	Rabbit	mono	E20	1:250-500	ab32516	Abcam
H3K9acetyl	Rabbit	mono	C5B11	1:1500	9649	Cell Signaling
$CD34^{+}$	Mouse	mono	QBEnd-10	1:50	M7165	Dako

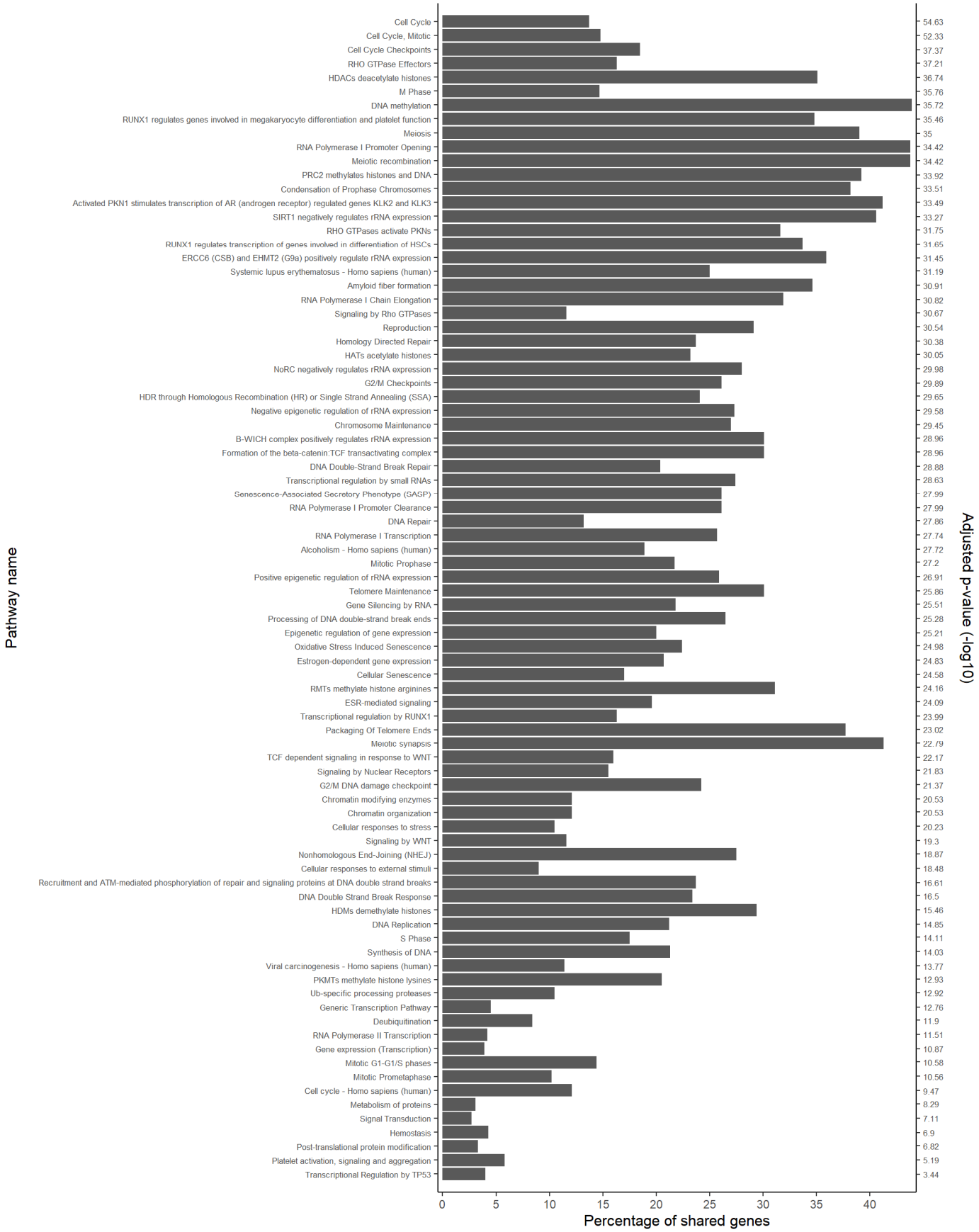

Figure S5a: Pathways significantly overrepresented in the DEGs between RD and PD. Over-representation analysis (ORA) made by ConsensusPathDB using DEGs (FDR <0.05, FC >0) with minimum overlap of 15 genes in pathway and p-value cut-off of 0.01. The percentage of DEGs associated with each biological process is shown along the x-axis and -log10-transformed p-values on the y-axis.

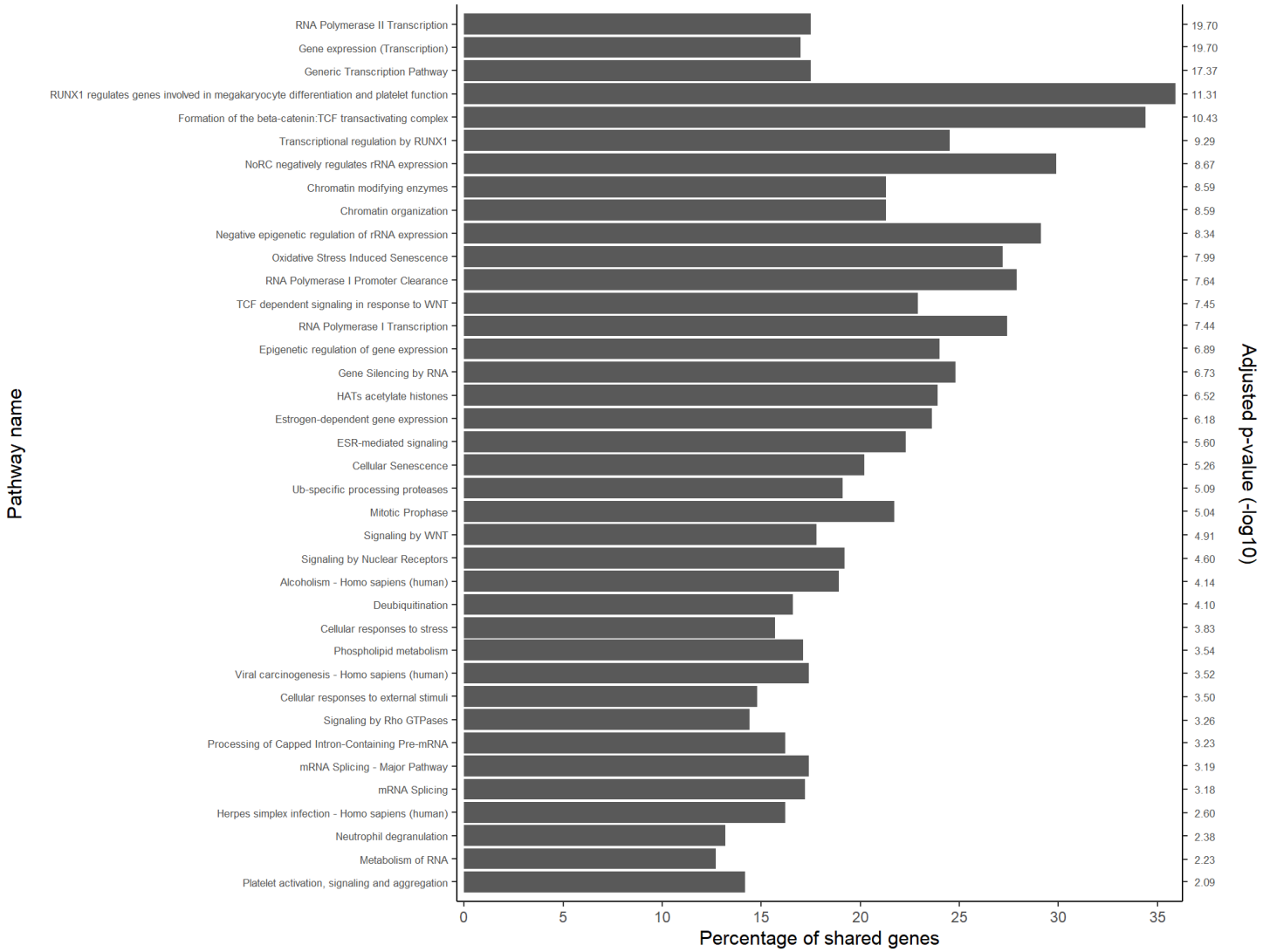

Figure S5b: Pathways significantly overrepresented in the DEGs between RD and CTRL. ORA made by ConsensusPathDB using DEGs (FDR <0.05, FC >0) with minimum overlap of 15 genes in pathway and p-value cut-off of 0.01. The percentage of DEGs associated with each biological process is shown along the x-axis and -log10-transformed p-values on the y-axis.


Pathway name
Adjusted p-value (-log10)
Gene expression (Transcription) 44.47
RNA Polymerase II Transcription 41.99
Generic Transcription Pathway 39.55
B-WICH complex positively regulates rRNA expression 37.61
DNA methylation 37.54
SIRT1 negatively regulates rRNA expression 37.07
Activated PKN1 stimulates transcription of AR (androgen receptor) regulated genes KLK2 and KLK3 36.25
RNA Polymerase I Promoter Opening 35.86
Meiotic recombination 35.86
Transcriptional regulation by small RNAs 34.53
Condensation of Prophase Chromosomes 34.47
PRC2 methylates histones and DNA 34.20
Cell Cycle, Mitotic 33.72
Negative epigenetic regulation of rRNA expression 33.08
NoRC negatively regulates rRNA expression 33.07
Positive epigenetic regulation of rRNA expression 32.72
Meiosis 32.69
Cell Cycle 32.64
RNA Polymerase I Chain Elongation 32.51
Formation of the beta-catenin:TCF transactivating complex 31.71
Telomere Maintenance 31.18
ERCC6 (CSB) and EHMT2 (G9a) positively regulate rRNA expression 30.98
Epigenetic regulation of gene expression 29.99
RUNX1 regulates transcription of genes involved in differentiation of HSCs 29.94
RUNX1 regulates genes involved in megakaryocyte differentiation and platelet function 29.86
RHO GTPases activate PKNs 29.85
Chromosome Maintenance 29.64
Gene Silencing by RNA 29.00
Oxidative Stress Induced Senescence 28.40
HDACs deacetylate histones 28.06
RNA Polymerase I Promoter Clearance 27.66
Amyloid fiber formation 27.39
RNA Polymerase I Transcription 27.07
Mitotic Prophase 26.47
Estrogen-dependent gene expression 26.33
ESR-mediated signaling 25.33
DNA Repair 24.57
Reproduction 24.23
HATs acetylate histones 24.18
M Phase 24.17
Systemic lupus erythematosus - Homo sapiens (human) 23.95
Packaging Of Telomere Ends 22.83
RMTs methylate histone arginines 22.34
Senescence-Associated Secretory Phenotype (SASP) 22.11
G2/M Checkpoints 21.90
Cellular Senescence 21.43
Transcriptional regulation by RUNX1 20.82
Signaling by Nuclear Receptors 19.28
TCF dependent signaling in response to WNT 18.73
DNA Double-Strand Break Repair 18.67
RHO GTPase Effectors 18.61
Chromatin modifying enzymes 18.49
Chromatin organization 18.49
Alcoholism - Homo sapiens (human) 17.97
Cell Cycle Checkpoints 17.27
Cellular responses to stress 17.15
Homology Directed Repair 16.37
Meiotic synapsis 16.32
Nonhomologous End-Joining (NHEJ) 15.95
Processing of DNA double-strand break ends 15.86
HDR through Homologous Recombination (HR) or Single Strand Annealing (SSA) 15.29
G2/M DNA damage checkpoint 14.91
Ub-specific processing proteases 13.96
Cellular responses to external stimuli 13.54
Signaling by WNT 13.34
Recruitment and ATM-mediated phosphorylation of repair and signaling proteins at DNA double strand breaks 13.34
mRNA Splicing - Major Pathway 13.29
Histone Modifications 13.13
DNA Double Strand Break Response 13.12

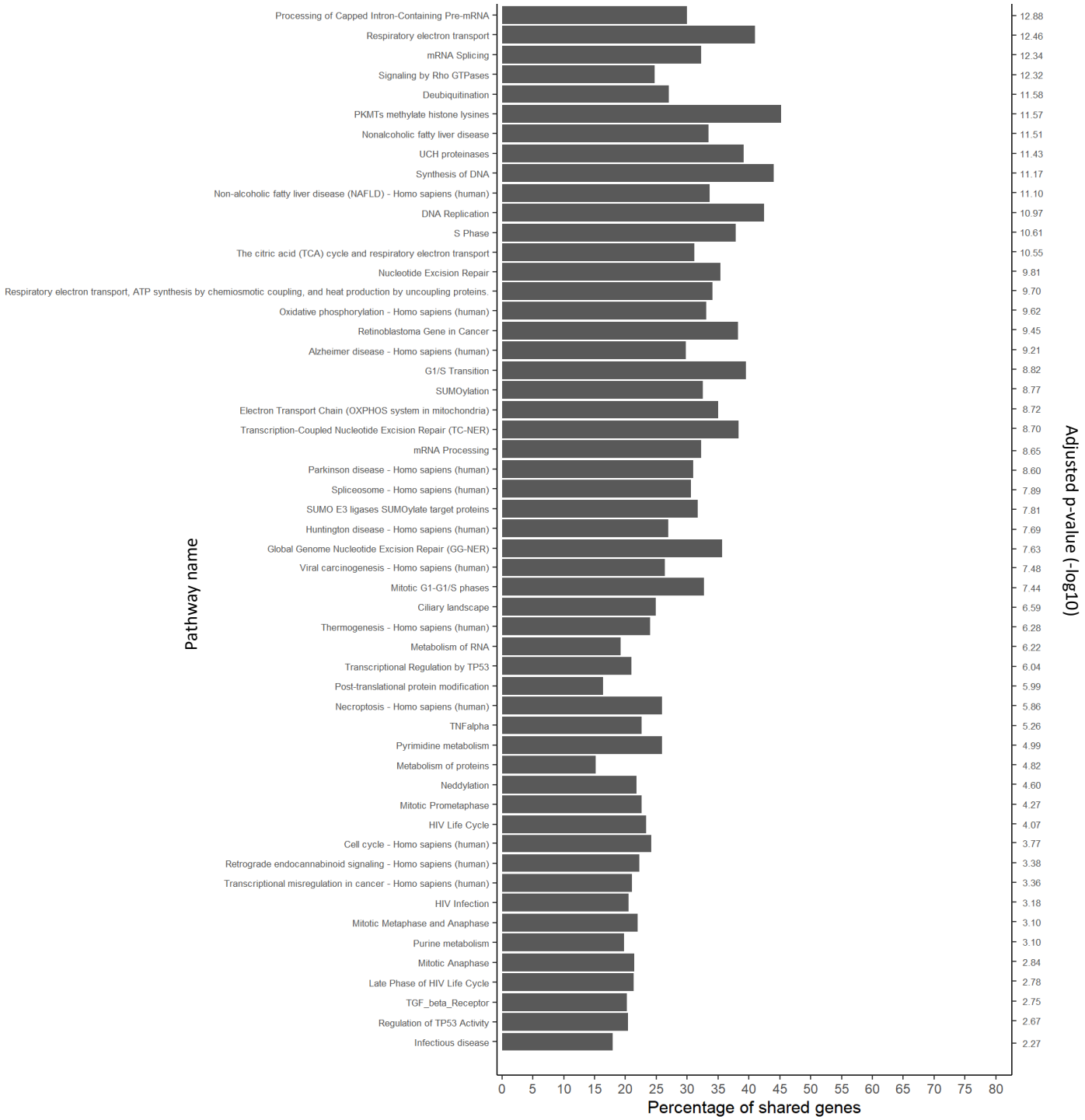

Figure S5c: Pathways significantly overrepresented in the DEGs between PD and CTRL. ORA made by ConsensusPathDB using DEGs (FDR <0.05, FC >0) with minimum overlap of 15 genes in pathway and p-value cut-off of 0.01. The percentage of DEGs associated with each biological process is shown along the x-axis and -log10-transformed p-values on the y-axis.

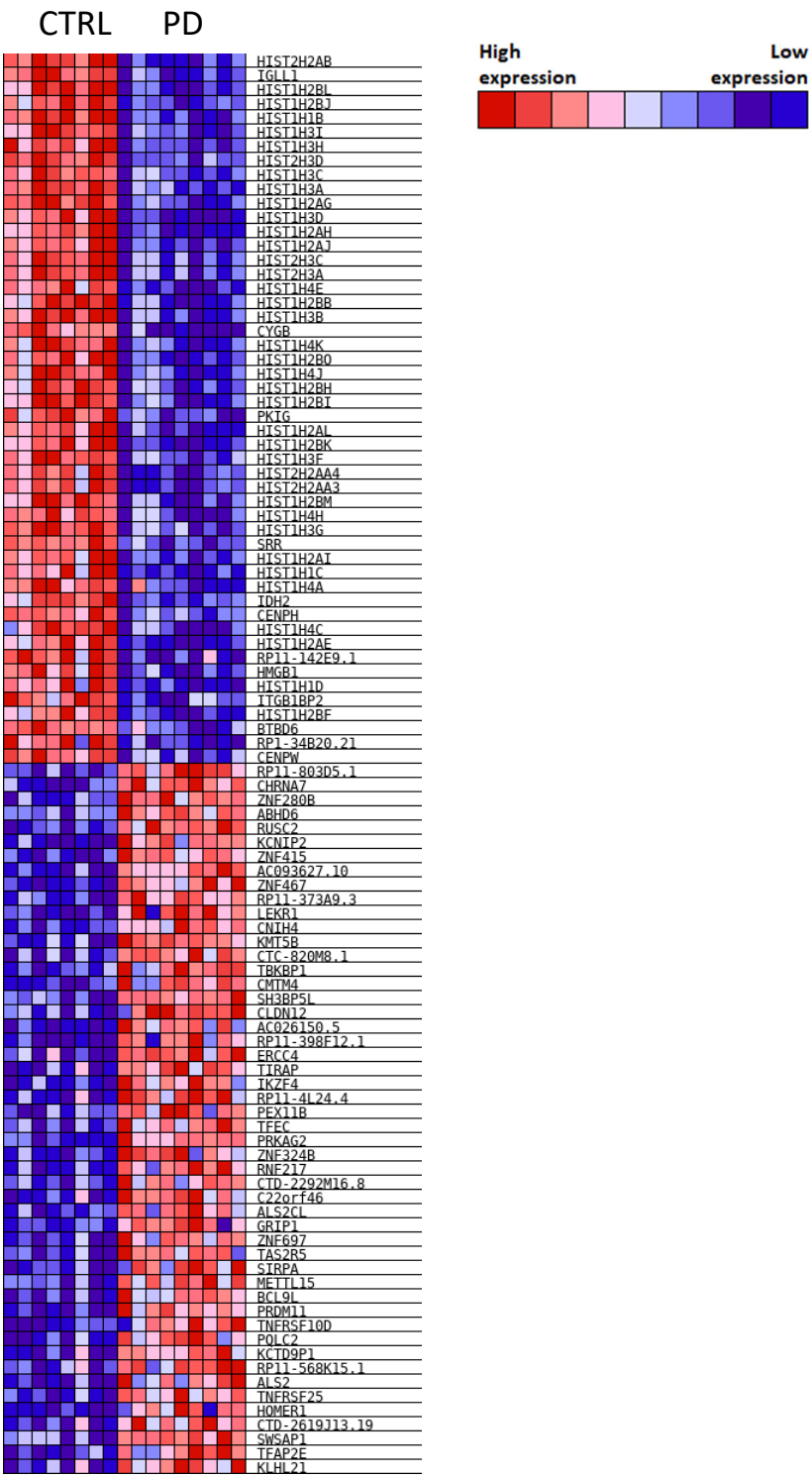

Figure S6: Heatmap of the top 50 up and downregulated genes in the PD vs. CTRL samples as identified by GSEA.

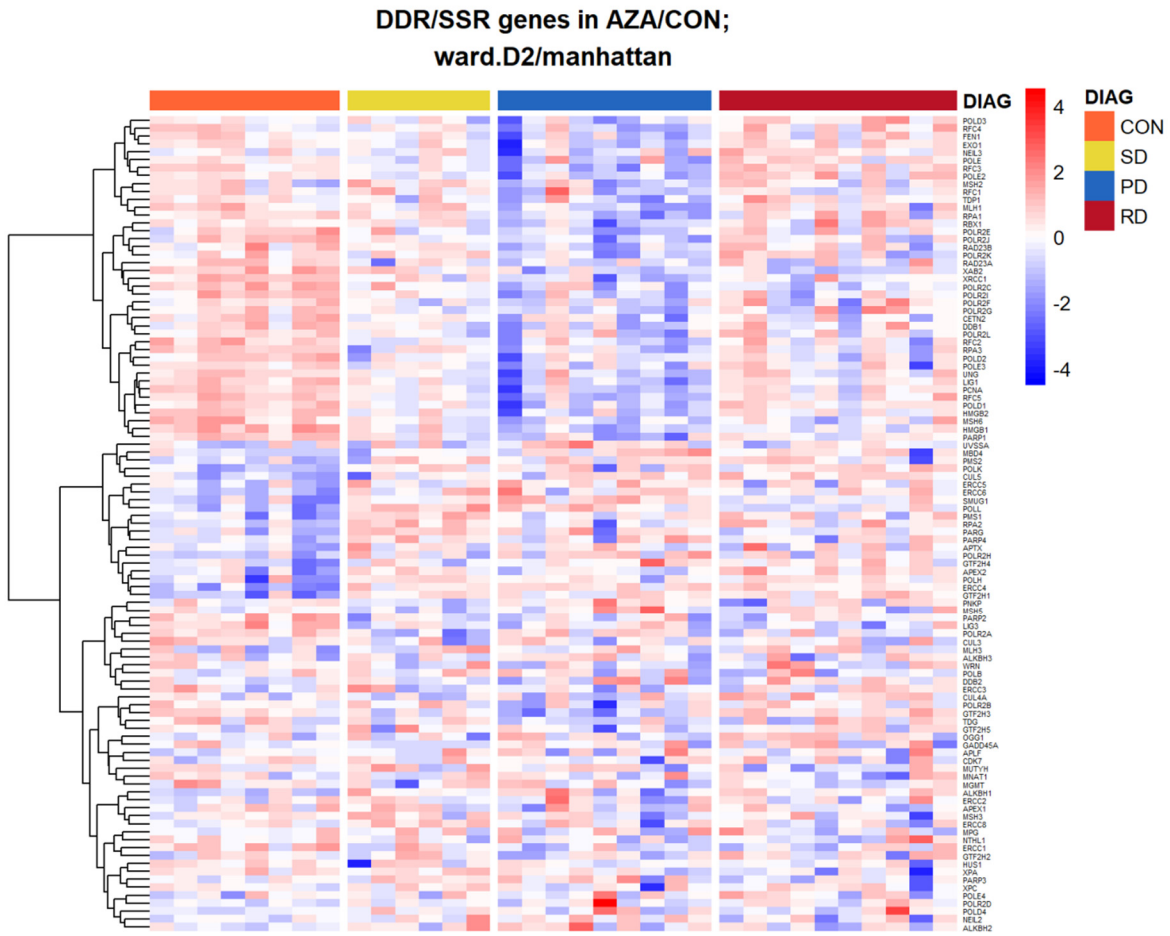

Figure S7a: Heatmap representation of differential expression of DNA single-strand break repair genes in the CD34⁺ HSPCs from AZA pre-treatment patients (RD, SD, PD) and normal controls (CON). The list of genes (n = 105) was adapted from Pearl et al (2015) [1].

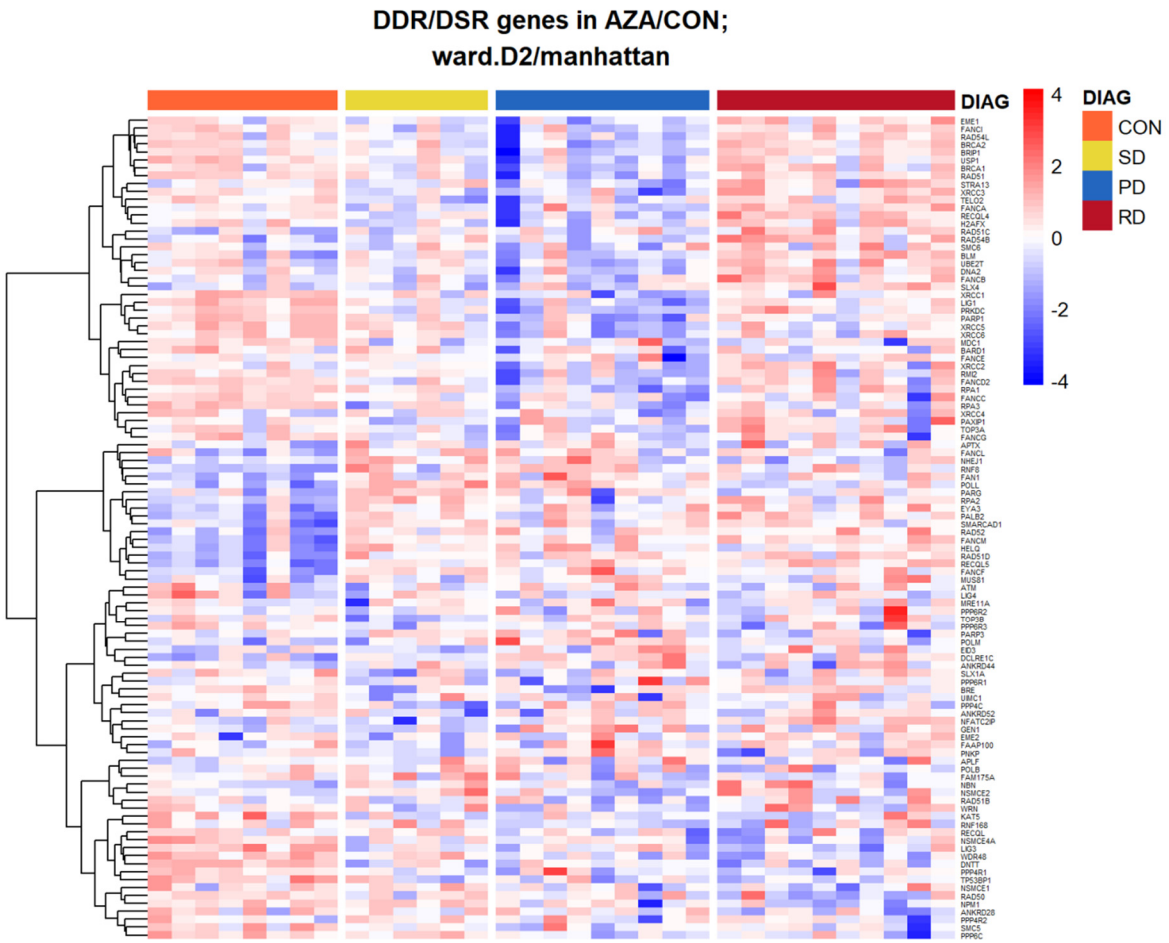

Figure S7b: Heatmap representation of differential expression of DNA double-strand break repair genes in the CD34⁺ HSPCs from AZA pre-treatment patients (RD, SD, PD) and normal controls (CON). The list of genes (n = 105) was adapted from Pearl et al (2015) [1].

Table S5: The top 10 up and downregulated DEGs between RD and PD. Up and downregulated genes are indicated in red and blue, respectively.

Upregulated DEGs					
Gene ID	**Gene symbol**	**LogFC**	**LogCPM**	**p-value**	**FDR**
ENSG00000196565	HBG2	4.153118783	4.120296678	0.00221902	0.0629817
ENSG00000213934	HBG1	4.148562311	4.135848035	0.002606297	0.06733715
ENSG00000163736	PPBP	3.868966411	6.790678829	0.000551591	0.033126168
ENSG00000101162	TUBB1	3.852763602	6.11622266	0.000143233	0.016810123
ENSG00000259207	ITGB3	3.558529841	7.604599917	0.000216148	0.020562717
ENSG00000284931	CTD-2643I7.4	3.523549238	4.117788735	0.011383826	0.139089305
ENSG00000119862	LGALSL	3.514399333	5.388804262	0.000150616	0.01703623
ENSG00000178732	GP5	3.416159009	3.765729738	0.000142354	0.016810123
ENSG00000137801	THBS1	3.414788869	8.336386456	0.00073137	0.037521876
ENSG00000173083	HPSE	3.331855749	4.84505582	7.36843E-06	0.003649912
Downregulated DEGs					
Gene ID	**Gene symbol**	**LogFC**	**LogCPM**	**p-value**	**FDR**
ENSG00000210082	MT-RNR2	-3.28969971	9.22991298	1.65084E-10	2.37144E-06
ENSG00000280800	CH507-513H4.6	-3.282208654	6.156719282	5.36197E-07	0.000600408
ENSG00000280614	CH507-513H4.4	-3.280686329	6.159268164	5.39059E-07	0.000600408
ENSG00000281181	CH507-513H4.3	-3.278352132	6.163105589	5.43356E-07	0.000600408
ENSG00000281383	CH507-513H4.5	-3.211821676	5.390666297	6.81518E-07	0.000699286
ENSG00000283458	RP11-1I2.1	-3.210937176	3.057280734	0.011005701	0.136972003
ENSG00000160321	ZNF208	-3.116835177	3.000686238	0.00460108	0.088746416
ENSG00000275215	RNA5-8SN4	-3.021873157	6.246345948	4.42778E-08	0.000160525
ENSG00000278233	RNA5-8SN3	-3.020919174	6.249364085	4.46989E-08	0.000160525
ENSG00000229236	TTTY10	-3.004284095	1.51872652	0.137565544	0.449371553

Table S6: Statistical analysis of differences in the levels of selected plasma metabolites between individual clinical groups of AZA-pre-treatment patients and normal controls.

CTRL	Citrate	cis-Aconitate	Isocitrate	α-KG	Succinate	Fumarate	Malate	L-2HG	D-2HG	3-PG	PEP	Lactate
PD	0.01 (*)	0.85	0.97	0.01 (*)	0.03 (*)	0.04 (*)	0.54	0.01 (*)	0.37	0.37	0.86	0.11
RD	0.73	0.73	0.33	0.82	0.18	0.01 (*)	0.11	0.02 (*)	0.08	0.15	0.79	0.22
SD	0.09	1.00	0.45	0.84	0.32	0.00(**)	0.01 (*)	0.20	0.32	0.41	0.62	0.03 (*)

PD	Citrate	cis-Aconitate	Isocitrate	α-KG	Succinate	Fumarate	Malate	L-2-HG	D-2-HG	3-PG	PEP	Lactate
CTRL	0.01 (*)	0.85	0.97	0.01 (*)	0.03 (*)	0.04 (*)	0.54	0.01 (*)	0.37	0.37	0.85	0.11
RD	0.01 (*)	0.44	0.51	0.10	0.22	0.44	0.51	0.86	0.65	0.57	1.00	0.96
SD	0.27	0.51	0.25	0.19	0.25	0.24	0.08	0.20	1.00	0.95	0.63	0.20

RD	Citrate	cis-Aconitate	Isocitrate	α-KG	Succinate	Fumarate	Malate	L-2-HG	D-2-HG	3-PG	PEP	Lactate
CTRL	0.73	0.73	0.33	0.82	0.18	0.01 (*)	0.11	0.02 (*)	0.08	0.15	0.79	0.22
PD	0.01 (*)	0.44	0.51	0.10	0.22	0.44	0.51	0.86	0.65	0.57	1.00	0.96
SD	0.17	0.83	0.98	0.95	0.98	0.78	0.27	0.30	0.51	0.40	0.63	0.25

SD	Citrate	cis-Aconitate	Isocitrate	α-KG	Succinate	Fumarate	Malate	L-2-HG	D-2-HG	3-PG	PEP	Lactate
CTRL	0.09	1.00	0.45	0.84	0.32	0.00(**)	0.01 (*)	0.20	0.32	0.41	0.62	0.03 (*)
RD	0.17	0.83	0.98	0.95	0.98	0.78	0.27	0.30	0.51	0.40	0.63	0.25
PD	0.27	0.51	0.25	0.19	0.25	0.24	0.08	0.20	1.00	0.95	0.63	0.20

The Mann Whitney U test, $p< 0.05$ (*), $p<0.001$ (**). The light –dark blue color scale indicates decreased metabolite level and the light – dark orange color scale shows increased metabolite level. Patients with *IDH2* mutations were excluded from the analyses. CTRL – controls, PD – progressive disease, RD – responders, SD – stable disease, α-KG – alpha-ketoglutarate, L- 2HG – L-2-hydroxyglutarate, D-2HG - D-2-hydroxyglutarate, 3-PG – 3-phosphoglycerate, PEP –phosphoenolpyruvate.

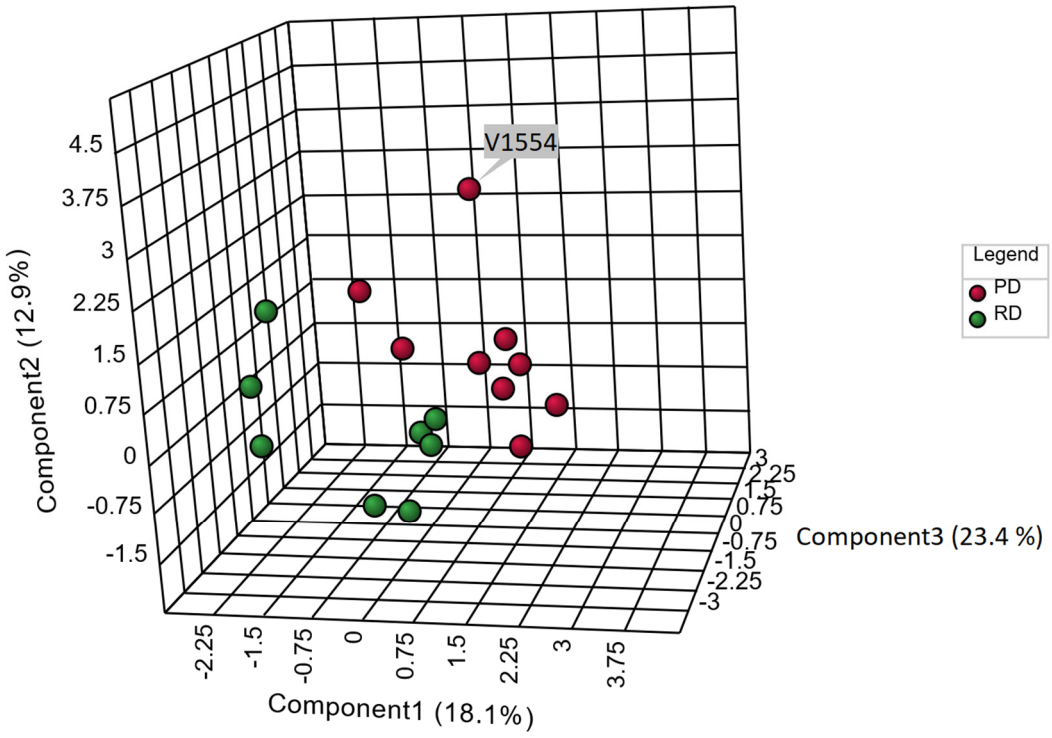

Figure S8a: Principal component analysis (PCA) of plasma metabolic profile of the AZA-pre-treatment PD and RD patients. A Patient with *IDH2* mutation is depicted by V1554 symbol. The samples were distinguished by a 19-metabolites signature (see **Supplementary Materials and Methods**).

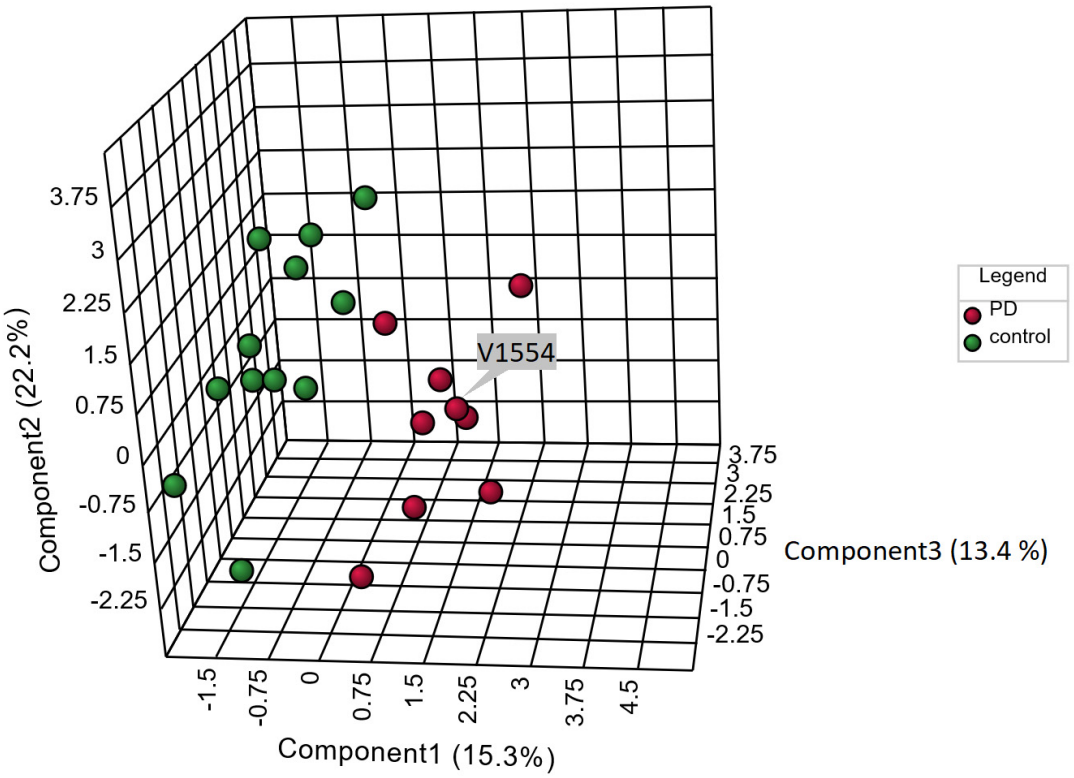

Figure S8b: PCA of plasma metabolic profile of the AZA-pre-treatment PD patients and normal controls. A Patient with *IDH2* mutation is depicted by V1554 symbol. The samples were distinguished by a 19-metabolites signature (see **Supplementary Materials and Methods**). PCA-3D plot displays a distinct profile between PD and CRTL samples.

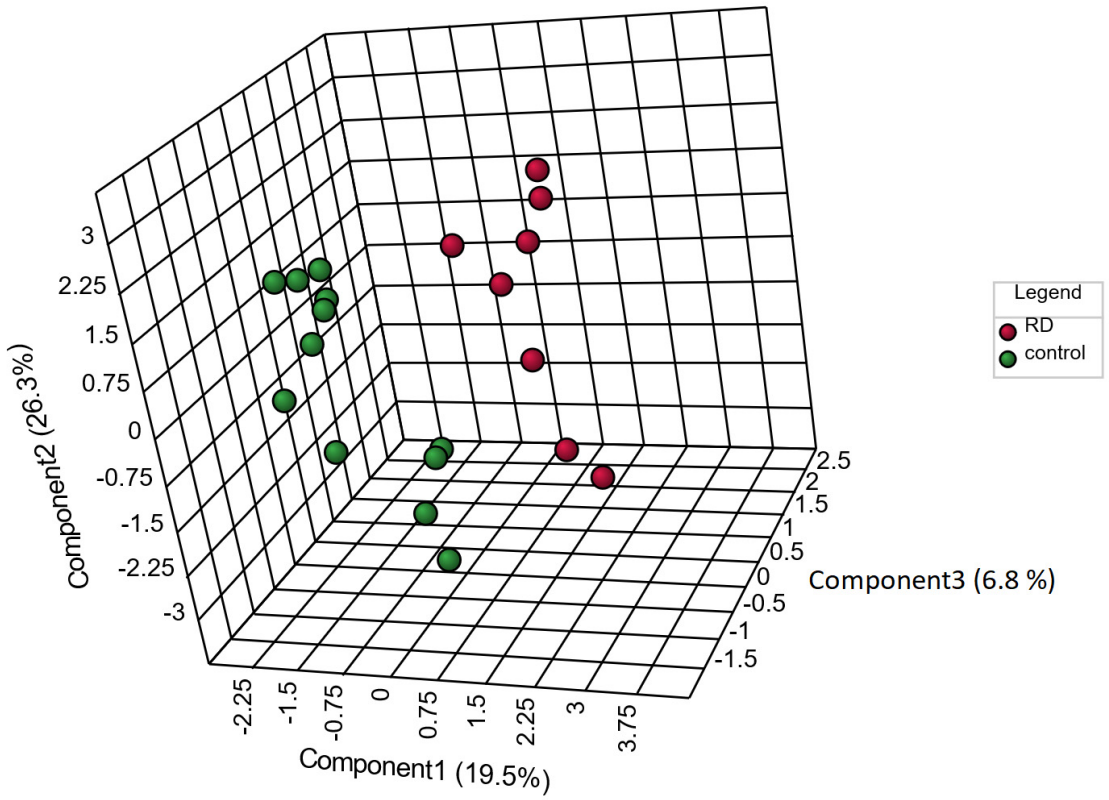

Figure S8c: PCA of plasma metabolic profile of the AZA-pre-treatment RD cohort and normal controls. The samples were distinguished by a 19-metabolites signature (see **Supplementary Materials and Methods**). PCA-3D plot displays a distinct profile between RD and CRTL samples.

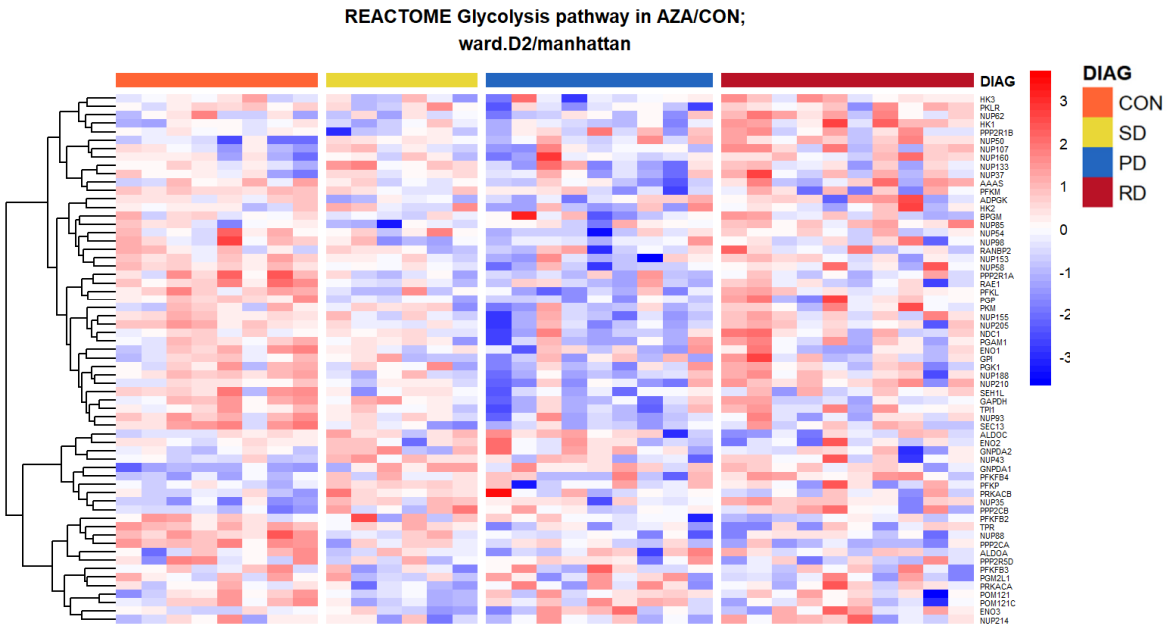

Figure S9: Heatmap visualization of gene expression profiles for glycolysis pathway genes (n = 63, Reactome) in the CD34⁺ HSPCs from AZA pre-treatment patients (RD, SD, PD) and normal controls (CON).

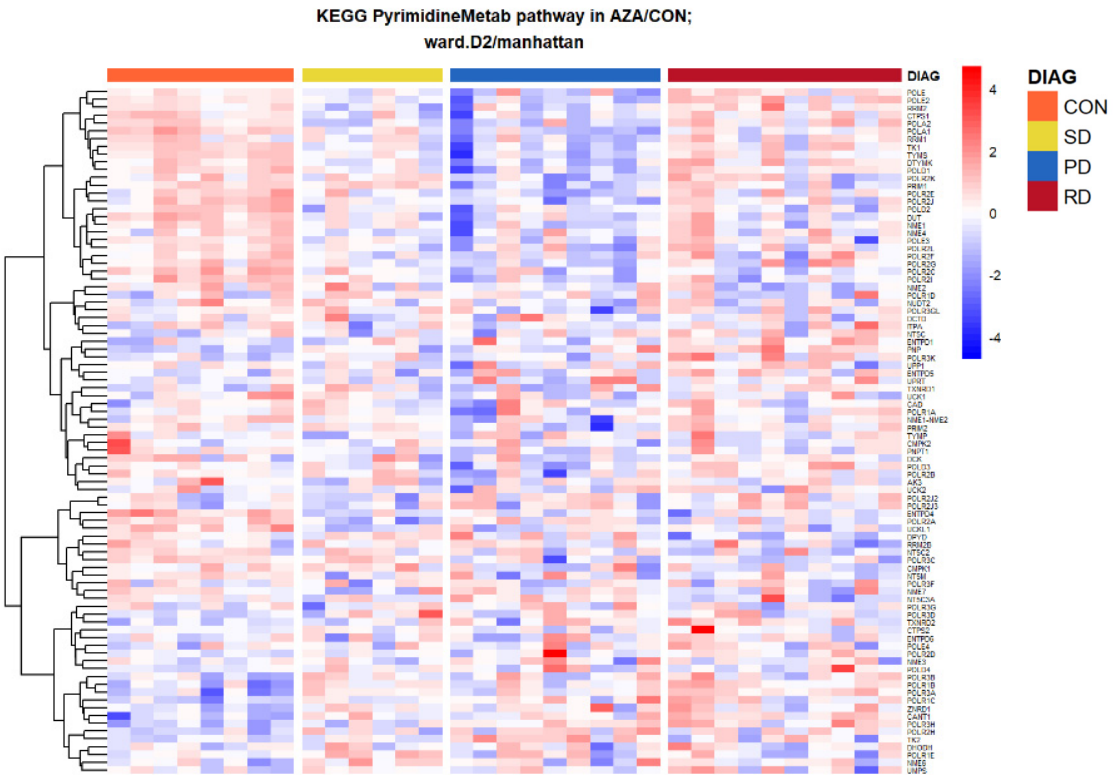

Figure S10: Heatmap visualization of gene expression profiles for pyrimidine metabolism genes (n = 88, KEGG) in the CD34⁺ HSPCs from AZA pre-treatment patients (RD, SD, PD) and normal controls (CON).

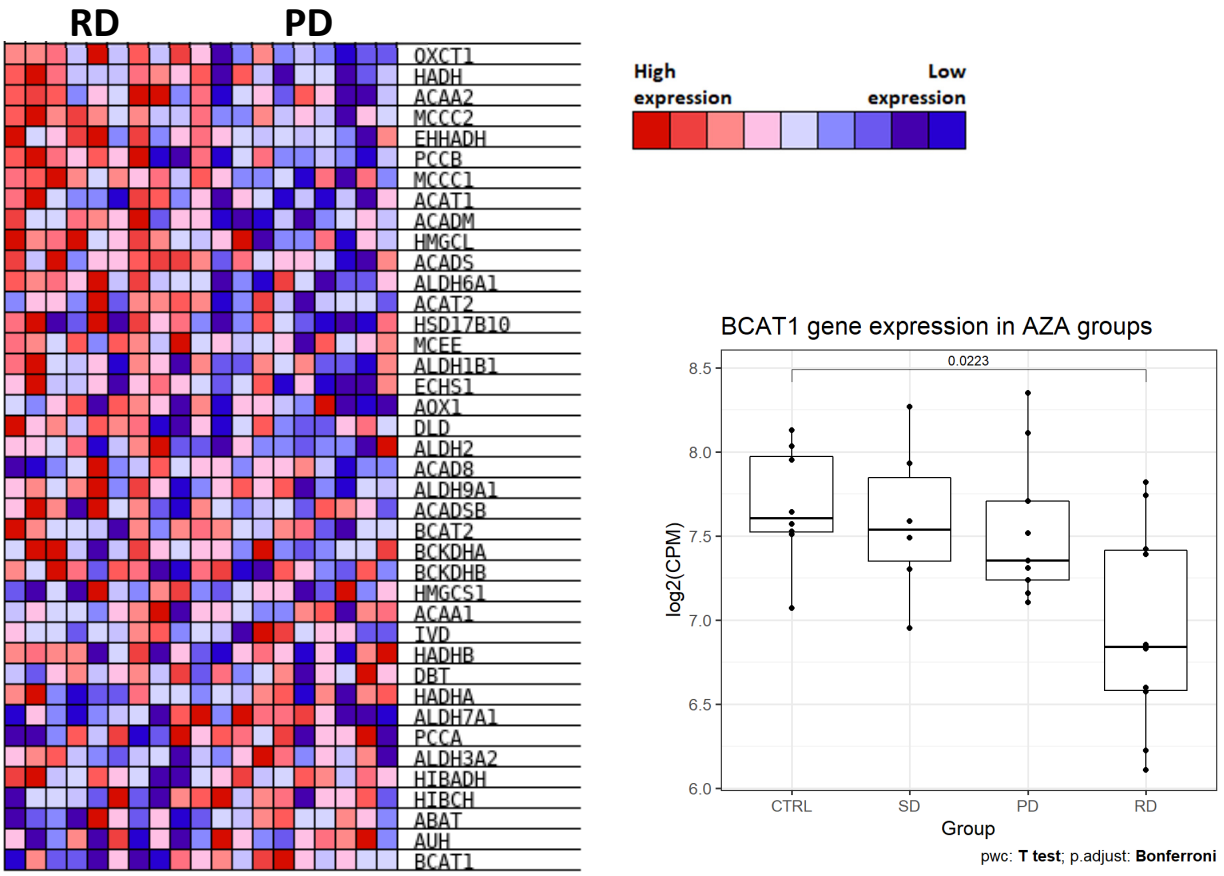

Figure S11: Left: Heatmap visualization of DEGs involved in valine/leucine/isoleucine degradation (n = 40, KEGG) in the $CD34^+$ HSPCs from AZA pre-treatment RD and PD patients. Right**:** The boxplot graph of relative log2 expression of *BCAT1* in the individual clinical groups (SD, PD, RD) of AZA-pre-treatment patients (n = 24) and normal controls (n = 8). Student's t-test with Bonferroni correction, p-value shown in the graph.

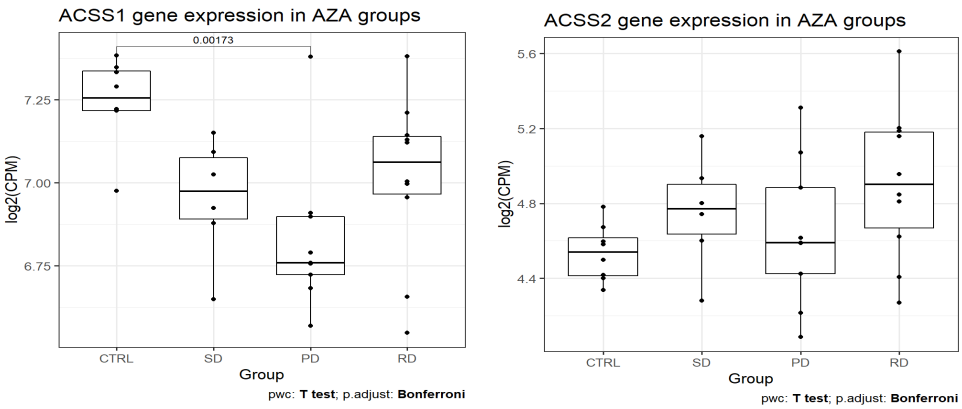

Figure S12: The boxplot graphs of relative log2 expression of *ACSS1* and *ACSS2* genes in the AZA-pre-treatment HSPCs from patients (n=24) and normal controls (n=8), Student's t-test with Bonferroni correction, p-value shown in the graphs.

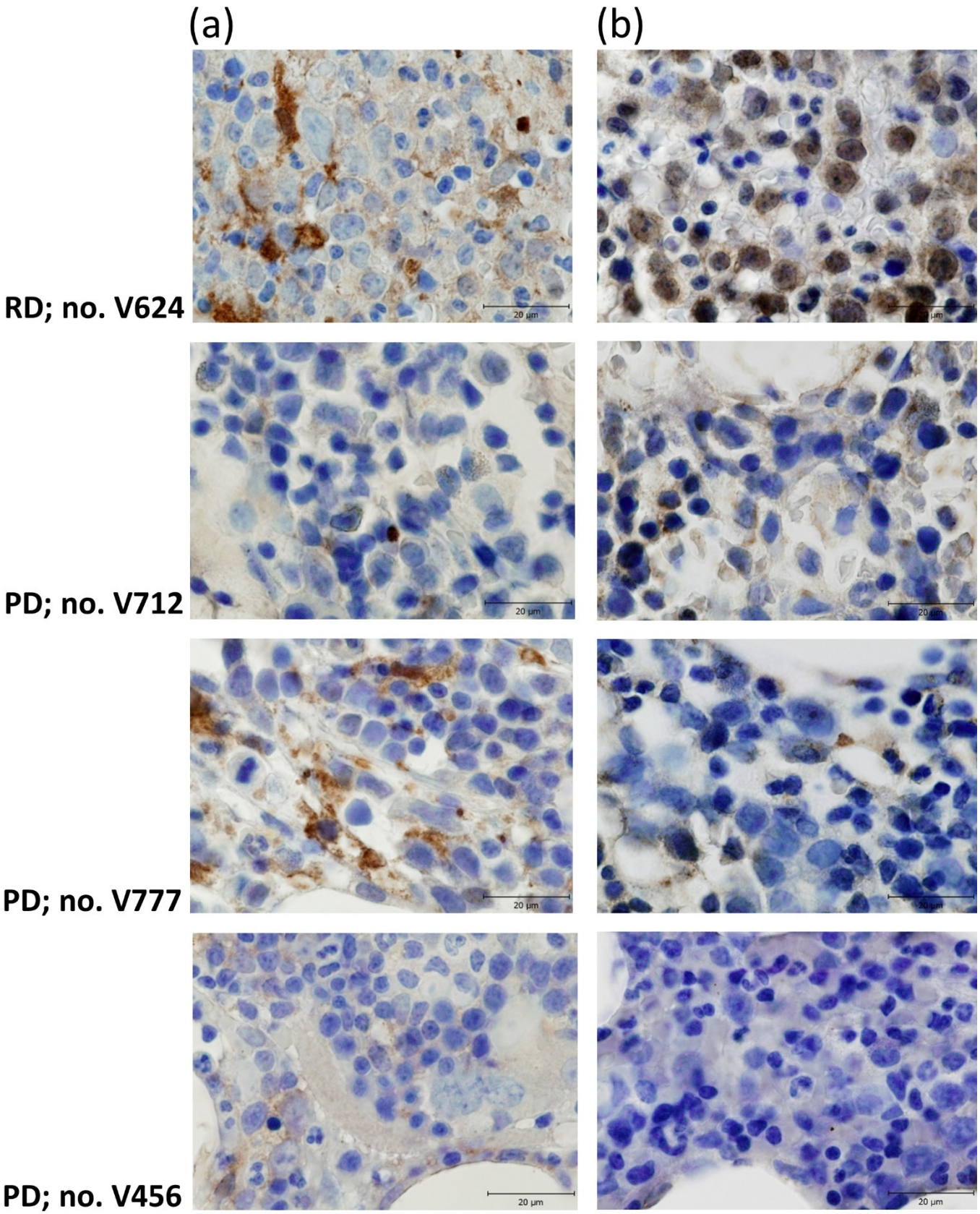

Figure S13: Immunohistochemistry (IHC) staining for IDH1 (a) and pan-acetyl lysine (b) in bone marrow trephine biopsies of MDS/AML-MRC patients. (a) Upper panel: Cytoplasmic staining for IDH1 in RD patient no. V624. Middle and lower panels: Weak/Intermediate cytoplasmic staining for IDH1 in three PD patients no. V712, V777, V456. (b) Nuclear pan-acetyl lysine staining in BM trephine biopsies from RD vs. PD patients. Upper panel: Strong nuclear staining documenting high level of lysine acetylation in RD patient no. V624. Middle and lower panels: Low/undetectable level of lysine acetylation in nuclei of three PD patients no. V712, V777, V456. See Supplementary Table S1 for patients' details. Scale bars, 20 µm.

Figure S14: The boxplot graph of relative log2 expression for *SIRT1* gene in the AZA-pre-treatment HSPCs from patients (n=24) and normal controls (n=8). Student's t-test with Bonferroni correction, p-values shown in the graph.

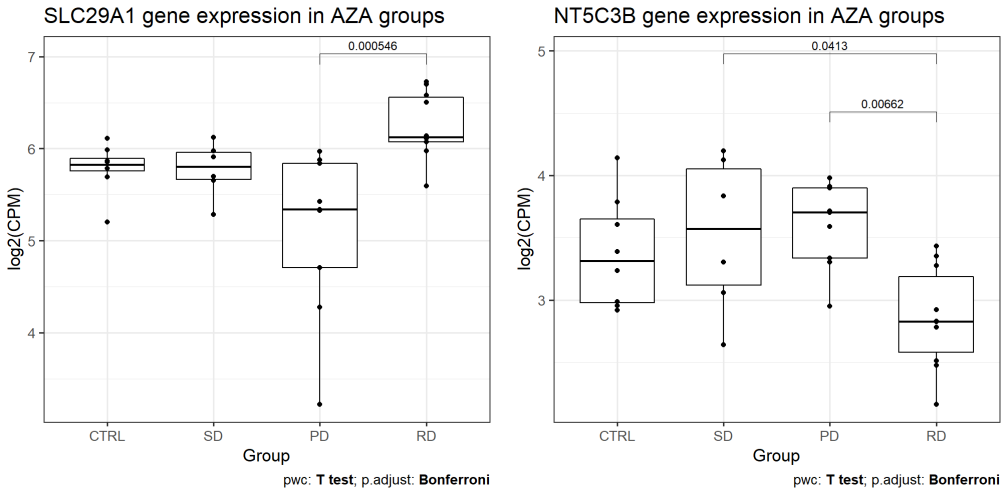

Figure S15: The boxplot graphs of relative log2 expression for *SLC29A1* and *NT5C3B* genes in the AZA-pre-treatment HSPCs from patients (n=24) and normal controls (n=8). Student's t-test with Bonferroni correction, p-values shown in the graphs.

Table S7: Distribution of myeloid and B-lymphoid subsets of $CD34^+$ cells in BM samples from 16 patients of discovery cohort, based on flow cytometry analysis. See Table S1 for patients' numbering and details.

Patient ID	% of **myeloid blasts** (CD45dim, $CD13^+$, $CD33^+$, $CD117^+$, $HLA\text{-}DR^+$) from total $CD34^+$ cells	% of **B-lymphoid precursors** (CD45dim, $CD10^+$, $CD19^+$, $CD20^-$) from total $CD34^+$ cells
V716	8	0
V1874	39	0
V1441	8.7	0
V1337	2.36	0.25
V1394	6	0
V1592	6.5	0
V714	17	0
V712	25	0
V1297	10	2.5
V1554	33	0
V344	18	1.8
V1788	29	0
V1456	2	1
V1884	12	0
V655	15	1.1
V1279	8	0

References:

1. Pearl, L.H.; Schierz, A.C.; Ward, S.E.; Al-Lazikani, B.; Pearl, F.M.G. Therapeutic Opportunities within the DNA Damage Response. *Nature Reviews Cancer* **2015**, *15*, 166–180, doi:10.1038/nrc3891.